

Hong-Ou-Mandel interferometer with one and two photon pairs

Olavo Cosme and S. Pádua*

Departamento de Física, Universidade Federal de Minas Gerais, Caixa Postal 702, Belo Horizonte, MG 30123-970, Brazil

Fabio A. Bovino

Elsag Datamat, via Puccini 2, Genova, Italy

A. Mazzei

Nano-Optics, Humboldt University, Hausvogteiplatz 5-6, D-10117 Berlin, Germany

Fabio Sciarrino

*Centro di Studi e Ricerche “Enrico Fermi,” via Panisperna 89/A, Compendio del Viminale, Roma 00184, Italy
Dipartimento di Fisica, Università “La Sapienza” and Consorzio Nazionale Interuniversitario per le Scienze Fisiche della Materia,
Roma 00185, Italy*

Francesco De Martini

*Dipartimento di Fisica, Università “La Sapienza” and Consorzio Nazionale Interuniversitario per le Scienze Fisiche della Materia,
Roma 00185, Italy**Accademia Nazionale dei Lincei, via della Lungara 10, Roma 00165, Italy*

(Received 9 October 2007; revised manuscript received 26 February 2008; published 30 May 2008)

We study the Hong-Ou-Mandel interferometer in the regime of spontaneous parametric down-conversion with high pump beam power at the crystal. In this regime one and two photons from a pump pulsed laser beam generate one and two pairs of photons, respectively. These photons are then directed to the beam splitter of the interferometer and detected at its exit in coincidence. An interesting phenomenon is observed: The reduction of the visibility of the Hong-Ou-Mandel coincidence peak (or dip) with the increase of pump power. We study the relation between the visibility of the fourth-order interference pattern and the power of the pumping laser beam for type I and type II phase-matching crystals. Our theoretical calculations are in good agreement with the experimental results.

DOI: [10.1103/PhysRevA.77.053822](https://doi.org/10.1103/PhysRevA.77.053822)

PACS number(s): 42.50.Dv, 42.65.-k, 42.25.Hz

I. INTRODUCTION

Quantum interference using a pair of correlated photons has played an important role in the recent developments of the fundamental study of quantum nonlocality [1–5]. Quantum interference with more than one pair is also a rich topic for research. For example, a more dramatic nonlocality violation with three particles is predicted [6,7]. Spontaneous parametric down-conversion (SPDC) became the most common source of two and four photons used in quantum optics and quantum-information experiments during the past 20 years. SPDC is a nonlinear optical process where one photon from the pump (p) laser beam incident to a crystal can originate two other photons: Signal (s) and idler (i) [8]. Quantum interference between single photons generated by independent sources [9] is essential for quantum-information processing schemes such as, for example, for implementing linear-optics quantum computers [10]. Interference with independent fields from parametric down-conversion was applied to quantum state teleportation where a two-photon entangled state is used to teleport an arbitrary unknown polarization state [11].

The photon pairs generated by the SPDC process are also called twin photons for being generated simultaneously with

a very small temporal uncertainty [12]. The usual way to determine the duration of a short pulse of light is to superimpose two similar pulses and measure the pulse overlapping with a device having a nonlinear response. In the regime of a few photons, the Hong-Ou-Mandel interferometer (HOM) was first developed as an interferometric tool for measuring the subpicosecond temporal uncertainty in the simultaneous photon pair generation by SPDC [12]. In their experiment, signal and idler photons with the same frequency and polarization are combined in a 50:50 beam splitter (BS) and the output photons are detected at the exit of the beam splitter by coincidence detection. When the idler and the signal paths from the crystal to the BS are made equal, no coincidence counts are detected at the BS output. The coincidence counts plotted as function of the idler-signal path difference shows then a dip. This interferometer has been used for tests of Bell inequalities [13], measurement of the tunneling time of photons [14], demonstration of the photon cancellation dispersion [15], demonstration of a quantum eraser [16], quantum teleportation [11], generation of a multiphoton state superposition [17], multimodal quantum interference [18], photon interferometry in cavities [19], construction of quantum logic gates for processing of quantum information [20], and cloning of a quantum state [21].

Nagasako *et al.* [22,23] studied the HOM dip with a single mode frequency theory when the light source is a parametric amplifier. Their main motivation was to use this

*spadua@fisica.ufmg.br

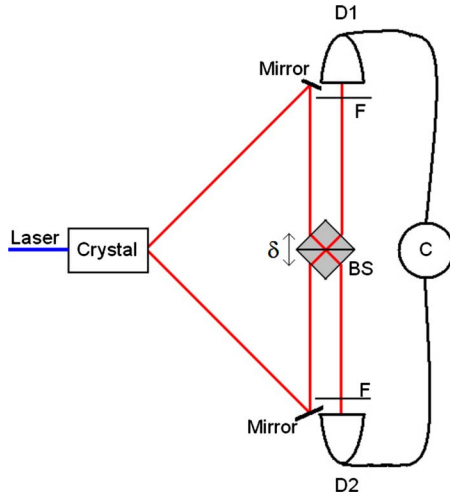


FIG. 1. (Color online) Hong-Ou-Mandel interferometer. BS is a 50:50 beam splitter, F is an interference filter, D_1 and D_2 are photon detectors, C is a coincidence detection system. The path length difference between the arms of the interferometer from the crystal to the BS (δ) is changed by displacing the BS.

interferometer for doing quantum lithography [24]. They showed that for beams incident to the BS with the same polarization, the vanishing of the coincidence rate disappears in the amplifier high gain limit.

In this work, we study theoretically and experimentally the HOM interferometer in the regime of strong pulse pump field at the crystal such that one and two pairs of photons per incident pump pulse can be generated by SPDC [25,26]. The two pairs or four photons are generated from two pump photons in a time interval smaller than the coincidence temporal window. HOM interference is studied theoretically in this regime for type I and type II phase-matching parametric down-conversion [27]. Dips or peaks can be obtained in the plot of the coincidence rate as a function of the signal-idler path difference when the incident photon pairs to the BS are in a triplet or singlet polarization state, respectively. A frequency multimode theory is used for obtaining the HOM interference pattern visibility as a function of the pump beam power. An experiment is done for type II phase matching, with photons generated in the polarization singlet state and is compared with the theoretical calculation. The nomenclature is based on Ref. [25] and a recent study [26].

II. HOM INTERFEROMETER WITH ONE AND TWO PHOTON PAIRS

The Hong-Ou-Mandel interferometer is represented in Fig. 1. A laser beam pumps the crystal generating one or two photon pairs per pump pulse that propagate in two different paths (a and b) in a noncollinear SPDC process. Depending on the one or two pair generation, we have one or two photons, respectively, in each path. Each beam is then directed to the 50:50 beam splitter by two mirrors and detected in coincidence at the exit of the beam splitter by a detection system with 3 ns of temporal resolution. Photons with the same frequency are selected by two identical interference filters

placed in front of the D_1 and D_2 detectors. Coincidence counts are measured as a function of the interferometer arm's difference δ produced by displacing the beam splitter (Fig. 1).

A. HOM interferometer with one and two pairs of photons and phase-matching type I

The process of spontaneous parametric down-conversion with the crystal pumped by a coherent pulse and generating one and two photon pairs by type I phase matching can be described by the following quantum state [8,25]:

$$|\Psi\rangle = M|\text{vac}\rangle + \eta E_p |\Phi_1\rangle + \eta^2 E_p^2 |\Phi_2\rangle, \quad (1)$$

where $\langle\Psi|\Psi\rangle=1$, $\langle\Phi_i|\Phi_j\rangle=\delta_{ij}$ ($i, j=1, 2$), E_p^2 is the number of photons of a pump pulse which fall on the crystal, M is a constant such that $M \gg \eta E_p$ ($M \lesssim 1$), ηE_p is the probability amplitude that one photon from the pump pulse is converted into two photons by SPDC, η^2 is the fraction of incident pump photons that are converted to signal-idler pairs and

$$|\Phi_1\rangle = \int d\omega_1 d\omega_2 \Phi(\omega_1, \omega_2) \hat{a}^\dagger(\omega_1) \hat{b}^\dagger(\omega_2) |\text{vac}\rangle, \quad (2)$$

$$|\Phi_2\rangle = \frac{1}{2} \int d\omega_1 d\omega_2 d\omega'_1 d\omega'_2 \Phi(\omega_1, \omega_2) \Phi(\omega'_1, \omega'_2) \hat{a}^\dagger(\omega_1) \hat{b}^\dagger(\omega_2) \hat{a}^\dagger(\omega'_1) \hat{b}^\dagger(\omega'_2) |\text{vac}\rangle. \quad (3)$$

In the above expression, a and b define idler and signal propagation modes, respectively; \hat{a}^\dagger and \hat{b}^\dagger are annihilation operators for photons in these modes. In the type I phase-matching condition, signal and idler photons have the same polarization. We assume that signal and idler propagation directions are well defined by apertures such that the photons are supposed to be single mode in momentum [8]. The spectral function $\Phi(\omega_1, \omega_2)$ which we assume to be symmetric with respect to ω'_1, ω'_2 , contains the phase-matching conditions for the SPDC, and incorporates the frequency dependence of the various factors present in the parametric interaction [8,25].

The state $|\Phi_1\rangle$ represents two photons converted from a photon of a pump pulse and the state $|\Phi_2\rangle$ represents four photons converted from two photons of a pump pulse when it crosses the crystal. The intensity operators for the times t_1 and t_2 , at the exit of the beam splitter (BS) (Fig. 1) are

$$\hat{\mathbf{I}}_1(t_1) = \frac{1}{2} \hat{\mathbf{F}}_a^{(-)}(t_1 + \delta) \cdot \hat{\mathbf{F}}_a^{(+)}(t_1 + \delta) + \frac{1}{2} \hat{\mathbf{F}}_a^{(-)}(t_1 + \delta) \cdot \hat{\mathbf{F}}_b^{(+)}(t_1) + \frac{1}{2} \hat{\mathbf{F}}_b^{(-)}(t_1) \cdot \hat{\mathbf{F}}_a^{(+)}(t_1 + \delta) + \frac{1}{2} \hat{\mathbf{F}}_b^{(-)}(t_1) \cdot \hat{\mathbf{F}}_b^{(+)}(t_1), \quad (4)$$

$$\hat{\mathbf{I}}_2(t_2) = \frac{1}{2} \hat{\mathbf{F}}_a^{(-)}(t_2) \cdot \hat{\mathbf{F}}_a^{(+)}(t_2) - \frac{1}{2} \hat{\mathbf{F}}_a^{(-)}(t_2) \cdot \hat{\mathbf{F}}_b^{(+)}(t_2 - \delta) - \frac{1}{2} \hat{\mathbf{F}}_b^{(-)}(t_2 - \delta) \cdot \hat{\mathbf{F}}_a^{(+)}(t_2) + \frac{1}{2} \hat{\mathbf{F}}_b^{(-)}(t_2 - \delta) \cdot \hat{\mathbf{F}}_b^{(+)}(t_2 - \delta), \quad (5)$$

where δ is the time delay between signal and idler photons.

This time delay is varied by displacing the BS in Fig. 1. The idler and signal electric field operators are

$$\hat{\mathbf{F}}_a^{(+)}(t) = \frac{1}{\sqrt{2\pi}} \int d\omega \hat{a}(\omega) e^{-i\omega t}, \quad (6)$$

$$\hat{\mathbf{F}}_b^{(+)}(t) = \frac{1}{\sqrt{2\pi}} \int d\omega \hat{b}(\omega) e^{-i\omega t}. \quad (7)$$

The probability of the coincidence detection after the BS is given for normal and temporal order [8] of the operators \hat{I}_1 and \hat{I}_2 , by

$$P_1(t_1, t_2) = \langle \mathcal{J} : \hat{\mathbf{I}}_1(t_1) \hat{\mathbf{I}}_2(t_2) : \rangle. \quad (8)$$

Then, by substituting (4) and (5) in (8), we obtain

$$P_1(t_1, t_2) = \frac{1}{4} \langle \hat{\mathbf{F}}_a^{(-)}(t_1 + \delta) \hat{\mathbf{F}}_b^{(-)}(t_2 - \delta) \hat{\mathbf{F}}_b^{(+)}(t_2 - \delta) \hat{\mathbf{F}}_a^{(+)}(t_1 + \delta) \rangle \quad (9)$$

$$+ \frac{1}{4} \langle \hat{\mathbf{F}}_b^{(-)}(t_1) \hat{\mathbf{F}}_a^{(-)}(t_2) \hat{\mathbf{F}}_a^{(+)}(t_2) \hat{\mathbf{F}}_b^{(+)}(t_1) \rangle \quad (10)$$

$$- \frac{1}{4} \langle \hat{\mathbf{F}}_a^{(-)}(t_1 + \delta) \hat{\mathbf{F}}_b^{(-)}(t_2 - \delta) \hat{\mathbf{F}}_a^{(+)}(t_2) \hat{\mathbf{F}}_b^{(+)}(t_1) \rangle \quad (11)$$

$$- \frac{1}{4} \langle \hat{\mathbf{F}}_b^{(-)}(t_1) \hat{\mathbf{F}}_a^{(-)}(t_2) \hat{\mathbf{F}}_a^{(+)}(t_2 - \delta) \hat{\mathbf{F}}_b^{(+)}(t_1 + \delta) \rangle \quad (12)$$

$$+ \frac{1}{4} \langle \hat{\mathbf{F}}_a^{(-)}(t_1) \hat{\mathbf{F}}_a^{(-)}(t_2) \hat{\mathbf{F}}_a^{(+)}(t_2) \hat{\mathbf{F}}_a^{(+)}(t_1) \rangle \quad (13)$$

$$+ \frac{1}{4} \langle \hat{\mathbf{F}}_b^{(-)}(t_1) \hat{\mathbf{F}}_b^{(-)}(t_2 - \delta) \hat{\mathbf{F}}_b^{(+)}(t_2 - \delta) \hat{\mathbf{F}}_b^{(+)}(t_1) \rangle. \quad (14)$$

The terms of the form $\langle \hat{\mathbf{F}}_a^{(-)} \hat{\mathbf{F}}_a^{(-)} \hat{\mathbf{F}}_b^{(+)} \hat{\mathbf{F}}_b^{(+)} \rangle$, $\langle \hat{\mathbf{F}}_a^{(-)} \hat{\mathbf{F}}_a^{(+)} \hat{\mathbf{F}}_a^{(+)} \hat{\mathbf{F}}_b^{(+)} \rangle$, $\langle \hat{\mathbf{F}}_a^{(-)} \hat{\mathbf{F}}_b^{(-)} \hat{\mathbf{F}}_b^{(+)} \hat{\mathbf{F}}_b^{(+)} \rangle$ and their Hermitian con-

jugates are nulls and, because of that, they do not appear above in $P_1(t_1, t_2)$. We obtain the coincidence rate by integrating the coincidence detection probability over times t_1 and t_2 in the time interval of the electronic window (usually on the order of 1 ns). This time interval is much larger than the longitudinal coherence time of the photons (on the order of 100 fs), so we can extend the integration interval to infinity. Some simplifications can be made in the above expressions. For instance, in the correlation functions (9)–(14) it is not necessary to discriminate the polarization indexes because, in the phase-matching type I, the generated photons have the same polarization. The terms (9) and (10) give the same contribution to the probability of detection and this can be seen if we exchange $t_1 + \delta$ for t_2 and $t_2 - \delta$ for t_1 . The term (11) is the Hermitian conjugate of (12), so they give the same contribution. The correlation functions (13) and (14) are the same when exchanged with $a \leftrightarrow b$ and $t_2 - \delta$ for t_2 . Since $\langle \Phi_1 | \Phi_2 \rangle = 0$, we can calculate the detection probability considering separately each term of the SPDC state and add the results at the end.

In this calculation we used the following commutation relations:

$$[\hat{a}(\omega), \hat{a}^\dagger(\omega')] = \delta(\omega - \omega'), \quad (15)$$

$$[\hat{a}(\omega), \hat{a}^\dagger(\omega') \hat{a}^\dagger(\omega'')] = \delta(\omega - \omega') \hat{a}^\dagger(\omega'') + \delta(\omega - \omega'') \hat{a}^\dagger(\omega'), \quad (16)$$

$$\begin{aligned} & [\hat{a}_s(\omega) \hat{a}_s(\omega'), \hat{a}_s^\dagger(\omega_1) \hat{a}_s^\dagger(\omega'_1)] \\ &= \delta(\omega - \omega_1) \delta(\omega' - \omega'_1) + \delta(\omega - \omega'_1) \delta(\omega' - \omega_1) \\ &+ \text{terms that annihilate the vacuum.} \end{aligned} \quad (17)$$

We also used

$$\int_{-\infty}^{\infty} e^{-i(\omega' - \overline{\omega}')t} dt = 2\pi \delta(\omega' - \overline{\omega}'). \quad (18)$$

After integrating the correlation functions (9)–(14) in t_1 and t_2 , we obtain the results shown below. The correlation functions (9) and (10) contribute to the coincidence rate with

$$\begin{aligned} & \eta^2 E_p^2 \int \int d\omega_1 d\omega_2 |\Phi(\omega_1, \omega_2)|^2 + 2\eta^4 E_p^4 \int \int d\omega_1 d\omega_2 |\Phi(\omega_1, \omega_2)|^2 \int \int d\omega'_1 d\omega'_2 |\Phi(\omega'_1, \omega'_2)|^2 \\ & + 2\eta^4 E_p^4 \int \int d\omega_1 d\omega_2 d\omega'_1 d\omega'_2 \Phi^*(\omega'_1, \omega_2) \Phi^*(\omega_1, \omega'_2) \Phi(\omega_1, \omega_2) \Phi(\omega'_1, \omega'_2), \end{aligned}$$

or

$$\eta^2 E_p^2 + 2E_p^4 (A + \varepsilon), \quad (19)$$

where

$$A = |\eta|^4 \int \int \int \int d\omega_1 d\omega_2 d\omega'_1 d\omega'_2 |\Phi(\omega_1, \omega_2) \Phi(\omega'_1, \omega'_2)|^2 = |\eta|^4 \quad (20)$$

is the accidental two-photon probability [25,26]. Indeed two uncorrelated fields 1 and 2 which excite, respectively, the detectors $D1$ and $D2$, can generate accidental coincidences which do not reflect any quantum correlation,

$$\varepsilon = |\eta|^4 \int d\omega_1 d\omega_2 d\omega'_1 d\omega'_2 \Phi(\omega_1, \omega_2) \Phi(\omega'_1, \omega'_2) \Phi^*(\omega_1, \omega'_2) \Phi^*(\omega'_1, \omega_2) \quad (21)$$

is the excess two-photon probability due to photon bunching [25,26]. For obtaining (19) and (20), we used $\langle \Phi_i | \Phi_j \rangle = \delta_{ij}$ ($i, j=1, 2$). The calculation of (9) is made in detail in the Appendix.

The correlation functions (11) and (12) contribute to the coincidence rate with

$$\begin{aligned} & \eta^2 E_p^2 \int \int d\omega_1 d\omega_2 |\Phi(\omega_1, \omega_2)|^2 e^{-i(\omega_1 - \omega_2)\delta} + \eta^4 E_p^4 \int \int \int \int d\omega_1 d\omega_2 d\omega'_1 d\omega'_2 |\Phi(\omega_1, \omega_2)|^2 |\Phi(\omega'_1, \omega'_2)|^2 e^{-i(\omega_1 - \omega_2)\delta} \\ & + \eta^4 E_p^4 \int \int \int \int d\omega_1 d\omega_2 d\omega'_1 d\omega'_2 \Phi(\omega_1, \omega_2) \Phi(\omega'_1, \omega'_2) \Phi^*(\omega_1, \omega'_2) \Phi^*(\omega'_1, \omega_2) e^{-i(\omega_1 - \omega'_2)\delta} \\ & + \eta^4 E_p^4 \int \int \int \int d\omega_1 d\omega_2 d\omega'_1 d\omega'_2 \Phi(\omega_1, \omega_2) \Phi(\omega'_1, \omega'_2) \Phi^*(\omega_2, \omega'_2) \Phi^*(\omega'_1, \omega_1) e^{-i(\omega_1 - \omega_2)\delta} \\ & + \eta^4 E_p^4 \int \int \int \int d\omega_1 d\omega_2 d\omega'_1 d\omega'_2 \Phi(\omega_1, \omega_2) \Phi(\omega'_1, \omega'_2) \Phi^*(\omega_2, \omega'_2) \Phi^*(\omega'_1, \omega_1) e^{-i(\omega_1 - \omega'_2)\delta} \end{aligned}$$

or, in another form

$$E_p^2 X(\delta) + E_p^4 [A(\delta) + \varepsilon(\delta) + \varepsilon'(\delta) + \varepsilon''(\delta)], \quad (22)$$

where

$$X(\delta) = |\eta|^2 \int \int d\omega_1 d\omega_2 |\Phi(\omega_1, \omega_2)|^2 e^{-i(\omega_1 - \omega_2)\delta}, \quad (23)$$

$$\begin{aligned} A(\delta) &= |\eta|^4 \int \int \int \int d\omega_1 d\omega_2 d\omega'_1 d\omega'_2 |\Phi(\omega_1, \omega_2)|^2 \\ &\times |\Phi(\omega'_1, \omega'_2)|^2 e^{-i(\omega_1 - \omega_2)\delta}, \quad (24) \end{aligned}$$

$$\begin{aligned} \varepsilon'(\delta) &= |\eta|^4 \int \int \int \int d\omega_1 d\omega_2 d\omega'_1 d\omega'_2 \Phi^*(\omega_1, \omega'_1) \Phi^*(\omega'_2, \omega_2) \\ &\times \Phi(\omega_1, \omega_2) \Phi(\omega'_1, \omega'_2) e^{-i(\omega_1 - \omega_2)\delta}, \quad (25) \end{aligned}$$

$$\begin{aligned} \varepsilon''(\delta) &= |\eta|^4 \int \int \int \int d\omega_1 d\omega_2 d\omega'_1 d\omega'_2 \Phi^*(\omega_1, \omega'_1) \\ &\times \Phi^*(\omega'_2, \omega_2) \Phi(\omega_1, \omega_2) \Phi(\omega'_1, \omega'_2) e^{-i(\omega_1 - \omega'_2)\delta}, \quad (26) \end{aligned}$$

and $\varepsilon(\delta)$ is obtained from ε [Eq. (21)] by multiplying the integrand by $e^{-i(\omega_1 - \omega'_2)\delta}$.

The correlation functions (13) and (14) contribute to the coincidence rate with

$$\begin{aligned} & |\eta|^4 E_p^4 \int d\omega_1 d\omega_2 d\omega'_1 d\omega'_2 [|\Phi(\omega_1, \omega_2) \Phi(\omega'_1, \omega'_2)|^2 \\ & + \Phi(\omega_1, \omega_2) \Phi(\omega'_1, \omega'_2) \Phi^*(\omega_1, \omega'_2) \Phi^*(\omega'_1, \omega_2)] \quad (27) \end{aligned}$$

or

$$E_p^4 (A + \varepsilon). \quad (28)$$

Finally the coincidences at the exit of the interferometer of Hong-Ou-Mandel, with two and four photons at the BS entrance generated by phase-matching type I, is

$$\begin{aligned} N_c &= \frac{E_p^2}{2} [X - X(\delta)] + \frac{E_p^4}{2} [3A - A(\delta)] \\ &+ \frac{E_p^4}{2} [3\varepsilon - \varepsilon(\delta) - \varepsilon'(\delta) - \varepsilon''(\delta)], \quad (29) \end{aligned}$$

where $X = X(0) = |\eta|^2$.

B. HOM interferometer with one and two pairs of photons and phase-matching type II

In the process of the SPDC when a crystal with phase-matching type II is pumped by a coherent pulse, the generated photons exit the crystal with orthogonal linear polarization. This process can be described by a state having the same form as the state shown in (1) but with [26]

$$\begin{aligned} |\Phi_1\rangle &= \frac{1}{\sqrt{2}} \int d\omega_1 d\omega_2 \Phi(\omega_1, \omega_2) \\ &\times [\hat{a}_H^\dagger(\omega_1) \hat{b}_V^\dagger(\omega_2) \pm \hat{a}_V^\dagger(\omega_1) \hat{b}_H^\dagger(\omega_2)] |\text{vac}\rangle, \quad (30) \end{aligned}$$

and

$$\begin{aligned} |\Phi_2\rangle &= \frac{1}{4} \int d\omega_1 d\omega_2 d\omega'_1 d\omega'_2 \Phi(\omega_1, \omega_2) \Phi(\omega'_1, \omega'_2) \\ &\times [\hat{a}_H^\dagger(\omega_1) \hat{b}_V^\dagger(\omega_2) \hat{a}_H^\dagger(\omega'_1) \hat{b}_V^\dagger(\omega'_2) \\ &\pm \hat{a}_H^\dagger(\omega_1) \hat{b}_V^\dagger(\omega_2) \hat{a}_V^\dagger(\omega'_1) \hat{b}_H^\dagger(\omega'_2) \\ &\pm \hat{a}_V^\dagger(\omega_1) \hat{b}_H^\dagger(\omega_2) \hat{a}_H^\dagger(\omega'_1) \hat{b}_V^\dagger(\omega'_2) \\ &+ \hat{a}_V^\dagger(\omega_1) \hat{b}_H^\dagger(\omega_2) \hat{a}_V^\dagger(\omega'_1) \hat{b}_H^\dagger(\omega'_2)] |\text{vac}\rangle, \quad (31) \end{aligned}$$

where H and V means horizontal and vertical polarization, respectively. We assume here that the photon pairs are generated in a singlet (minus sign) or triplet (plus sign) polarization entangled state. The intensity operators at the detectors $D1$ and $D2$ are equal to the operators shown in the expressions (4) and (5), except that now we must sum the right-hand side of these expressions in H and V , for each mode a and b . The probability of coincidence at the beam-splitter exit of the HOM interferometer for phase-matching type II [8] is then calculated from expression (8),

$$P_{II}(t_1, t_2) = \frac{1}{4} \sum_{i=H,V} \sum_{j=H,V} [\langle \hat{\mathbf{F}}_{ai}^{(-)}(t_1 + \delta) \hat{\mathbf{F}}_{bj}^{(-)}(t_2 - \delta) \hat{\mathbf{F}}_{bj}^{(+)}(t_2 - \delta) \hat{\mathbf{F}}_{ai}^{(+)}(t_1 + \delta) \rangle \quad (32)$$

$$+ \langle \hat{\mathbf{F}}_{bi}^{(-)}(t_1) \hat{\mathbf{F}}_{aj}^{(-)}(t_2) \hat{\mathbf{F}}_{aj}^{(+)}(t_2) \hat{\mathbf{F}}_{bi}^{(+)}(t_1) \rangle \quad (33)$$

$$+ \langle \hat{\mathbf{F}}_{ai}^{(-)}(t_1) \hat{\mathbf{F}}_{aj}^{(-)}(t_2) \hat{\mathbf{F}}_{aj}^{(+)}(t_2) \hat{\mathbf{F}}_{ai}^{(+)}(t_1) \rangle \quad (34)$$

$$+ \langle \hat{\mathbf{F}}_{bi}^{(-)}(t_1) \hat{\mathbf{F}}_{bj}^{(-)}(t_2 - \delta) \hat{\mathbf{F}}_{bj}^{(+)}(t_2 - \delta) \hat{\mathbf{F}}_{bi}^{(+)}(t_1) \rangle \quad (35)$$

$$- \langle \hat{\mathbf{F}}_{ai}^{(-)}(t_1 + \delta) \hat{\mathbf{F}}_{bj}^{(-)}(t_2 - \delta) \hat{\mathbf{F}}_{aj}^{(+)}(t_2) \hat{\mathbf{F}}_{bi}^{(+)}(t_1) \rangle \quad (36)$$

$$- \langle \hat{\mathbf{F}}_{bi}^{(-)}(t_1) \hat{\mathbf{F}}_{aj}^{(-)}(t_2) \hat{\mathbf{F}}_{aj}^{(+)}(t_2 - \delta) \hat{\mathbf{F}}_{bi}^{(+)}(t_1 + \delta) \rangle, \quad (37)$$

where

$$\hat{\mathbf{F}}_{ai}^{(+)}(t) = \frac{1}{\sqrt{2\pi}} \int d\omega \hat{a}_i(\omega) e^{-i\omega t}, \quad (38)$$

$$\hat{\mathbf{F}}_{bi}^{(+)}(t) = \frac{1}{\sqrt{2\pi}} \int d\omega \hat{b}_i(\omega) e^{-i\omega t}. \quad (39)$$

Here, as mentioned above in the type I case, some of the correlation functions are not shown in the expressions (32)–(37) because they are null. The coincidence rate is calculated as

$$N_{IIc}(\delta) = \int_{-\infty}^{\infty} \int_{-\infty}^{\infty} P_{II}(t_1, t_2) dt_1 dt_2. \quad (40)$$

The contribution of (32) and (33) to the coincidence rate when the indexes are $i=j=H$ or $i=j=V$ is

$$\begin{aligned} & \frac{\eta^4 E_p^4}{4} \int \int \int \int d\omega_1 d\omega_2 d\omega'_1 d\omega'_2 |\Phi(\omega_1, \omega_2)|^2 |\Phi(\omega'_1, \omega'_2)|^2 \\ & = \frac{E_p^4}{4} A, \end{aligned} \quad (41)$$

and, when the indexes are $i=H, j=V$ or $i=V, j=H$ is

$$\frac{E_p^2}{2} X + E_p^4 A + \frac{E_p^4}{2} \varepsilon. \quad (42)$$

The total contribution of the correlation functions (32) and (33) is

$$E_p^2 X + 2E_p^4 A + E_p^4 \varepsilon. \quad (43)$$

The terms (34) and (35), when the indexes are $i=j=H$ or $i=j=V$, are equal to

$$\frac{E_p^4}{4} (A + \varepsilon) \quad (44)$$

and, when the indexes are $i=H, j=V$ or $i=V, j=H$, are equal to

$$\frac{E_p^4}{4} A. \quad (45)$$

The total contribution of (34) and (35) to the number of coincident photons is thus

$$\frac{E_p^4}{2} (2A + \varepsilon). \quad (46)$$

In a similar way, (36) and (37), when the indexes are $i=j=H$ or $i=j=V$, give

$$\frac{E_p^4}{4} \varepsilon''(\delta) \quad (47)$$

and, when the indexes are $i=H, j=V$ or $i=V, j=H$ result in

$$\pm \left(\frac{E_p^2}{2} X(\delta) + \frac{E_p^4}{2} A(\delta) + \frac{E_p^4}{4} \varepsilon(\delta) + \frac{E_p^4}{4} \varepsilon'(\delta) \right). \quad (48)$$

The total contribution of the correlation functions (36) and (37) to coincidences is

$$\pm \left(\frac{E_p^2}{2} X(\delta) + \frac{E_p^4}{2} A(\delta) + \frac{E_p^4}{2} \varepsilon(\delta) + \frac{E_p^4}{2} \varepsilon'(\delta) \right) + \frac{E_p^4}{2} \varepsilon''(\delta). \quad (49)$$

Finally, the number of coincident photons at the exit of the Hong-Ou-Mandel interferometer with two and four photons exiting the crystal by SPDC phase-matching type II, is

$$\begin{aligned} N_c(\delta) &= \frac{E_p^2}{2} [X \mp X(\delta)] + \frac{E_p^4}{2} [3A \mp A(\delta)] \\ &+ \frac{E_p^4}{4} [3\varepsilon \mp \varepsilon(\delta) \mp \varepsilon'(\delta) - \varepsilon''(\delta)], \end{aligned} \quad (50)$$

where the plus signs in (50) are the coincidences when photon pairs are generated in a singlet state while the minus sign is for the case where the photon pairs are generated in a triplet state.

III. EXPERIMENTAL RESULTS

The HOM interferometer scheme is shown in Fig. 1. We have tested experimentally the calculated HOM interference pattern as a function of the average pump beam power at the crystal. The laser beam source used in the setup is a regenerative amplifier (RegATM-coherent) producing at its output 200 fs light pulses with a repetition rate of $N=250$ KHz. The seed pulsed beam to the amplifier comes from a mode locked

200 fs laser (Mira™-Coherent) with repetition rate of 76 MHz and operating at 795 nm. The pump uv beam at 397.5 nm is produced by second harmonic generation after the infrared RegA pulsed beam is sent to a 1.0 mm type I β -barium borate (BBO) crystal. The average power of the pulsed uv beam is 150 mW and is directed to a 1.5 mm BBO crystal for the SPDC generation with type II phase matching. The uv beam is slightly focused to the crystal by a 1.0 m focal length lens. Due to the high energy per pump pulse at the crystal, one and two photon pairs in the singlet state are generated by SPDC from one and two photons of the pump pulse, respectively. Photons with the same frequency $\omega_1 = \omega_2 \approx \frac{\omega_0^c}{2}$ exit the crystal making an angle of 2.5° with the pump beam direction and are selected by two pinholes with 1.5 mm diameter placed in their paths. The photon pairs are generated in a polarization singlet state by the scheme shown in Ref. [28]. The photon pairs are then directed to the 50:50 beam splitter as shown in Fig. 1. By displacing the BS with a translation stage coupled to a step motor we can balance photons 1 (signal) and 2 (idler) paths, without losing the interferometer aligning. Both detectors $D1$ and $D2$ are avalanche photodiodes (Perkin-Elmer-SPCM-AQR-14) operating in photon counting mode and $F1, F2$ are interference filters placed in front of them, with 3.0 nm full width at half-maximum (FWHM) bandwidth and centered at 795 nm. The coincidence rate is measured by a coincidence circuit with 3 ns temporal resolution.

We assume that the spectral distribution of the photons' wave packets is determined by the filter's frequency distribution, because the gain frequency bandwidth of the parametric down-conversion process and the frequency bandwidth of the pump field spectrum are much broader than the filter bandwidth [12,25]. By considering the transmission function of the two filters to be Gaussian and centered at $\omega_1 \approx \frac{\omega_0^c}{2}$ and $\omega_2 \approx \frac{\omega_0^c}{2}$, we can write the state spectral function as

$$\Phi(\omega_1, \omega_2) = \Phi\left(\omega_1 = \frac{\omega_0^c}{2}, \omega_2 = \frac{\omega_0^c}{2}\right) f(\omega_1) f(\omega_2) \quad (51)$$

with

$$f(\omega) = \frac{1}{\sqrt{\Delta\omega_f \sqrt{\pi}}} \exp\left(-\frac{\left(\omega - \frac{\omega_0^c}{2}\right)^2}{2\Delta\omega_f^2}\right). \quad (52)$$

$\Delta\omega_f$ is the FWHM of the interference filter. By substituting (51) in (50), we obtain the following expression for the number of coincidence photons at the HOM interferometer exit for photon pairs in the singlet state,

$$N_c(\delta) = \frac{E^2}{2} X_0 (1 + e^{-(\Delta\omega_f)^2 \delta^2}) + \frac{E^4}{4} (2A_0 + \varepsilon_0) (3 + e^{-(\Delta\omega_f)^2 \delta^2}) \quad (53)$$

with $X_0 = X(0)$, $A_0 = A(0)$, and $\varepsilon_0 = \varepsilon(0)$. For testing the calculated HOM output coincidence rate for the singlet state we need to determine the quantities X_0 and $(2A_0 + \varepsilon_0)$. We describe below the experimental procedure used for obtaining

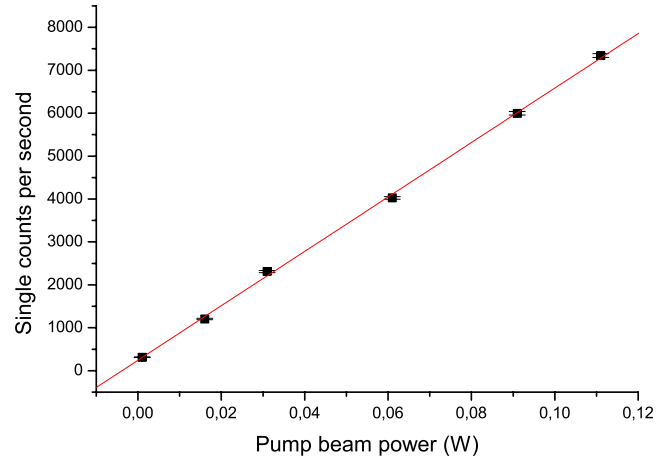


FIG. 2. (Color online) Single counts in one of the detectors in terms of the average pump beam power. The experimental slope of the straight line is $(63.6 \pm 0.8) \times 10^3$ photons/s W. From it we can obtain a measurement of the detector efficiency times X_0 .

them. All experimental plots are done in terms of the average pump beam power P that is proportional to the theoretical quantity E_p^2 . $E_p^2 = \frac{P}{N h \nu}$, where N is the pump laser repetition rate, ν is the pump beam frequency, and h is the Planck constant [29].

We obtained X_0 by plotting the single counts of one of the detectors at the exit of the interferometer as a function of the average pump beam power. The probability rate of detecting a photon in the signal or idler field is given by [25]

$$P(t_j) = \langle \hat{\mathbf{I}}(t_j) \rangle$$

with $j=1, 2$. This quantity can easily be calculated by using the state shown in Eq. (2). The overall probability of detecting a photon is obtained by integrating $P(t_j)$ in all times as discussed above,

$$\begin{aligned} P_{1j} &= \int_{-\infty}^{\infty} P(t_j) dt_j = E_p^2 |\eta|^2 \iint d\omega_1 d\omega_2 |\Phi(\omega_1, \omega_2)|^2 \\ &= E_p^2 X(0), \end{aligned} \quad (54)$$

where we used the normalization condition $\langle \Psi | \Psi \rangle = 1$ for evaluating the integral. Therefore, $E_p^2 X(0)$ is the probability of a single photon conversion in a single pump pulse. When we consider the efficiency α_j of the detector and the laser beam repetition rate N , we have the following expression for the single counts:

$$R_{1j} = N \alpha_j E_p^2 X_0 = \alpha_j X_0 \frac{P}{h \nu}. \quad (55)$$

The single counts per second in terms of the average pump beam power is shown in Fig. 2. The experimental slope of the straight line is $(63.6 \pm 0.8) \times 10^3$ photons/s W. From it we can obtain a measurement of the detector efficiency times X_0 .

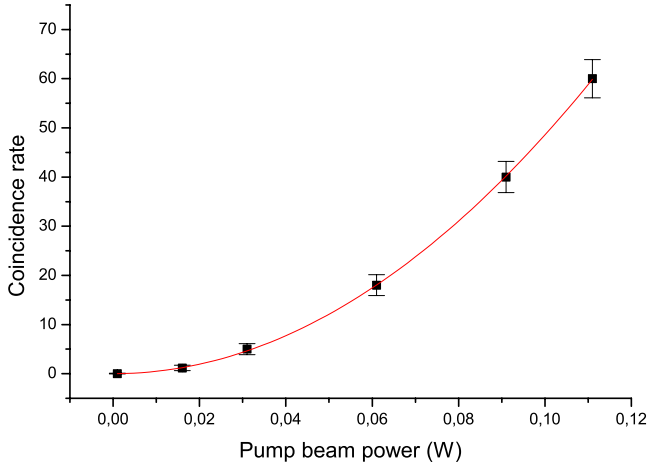


FIG. 3. (Color online) Coincidence rate in terms of the average pump beam power, with one of the arms of the interferometer blocked, and detected at the exit of the BS. The continuous curve is an experimental fit done with the function cP^d ; $c=(4.9 \pm 0.2) \times 10^3$ photons/s W^2 and $d=2.00 \pm 0.02$ [see Eq. (56)]. We determine from c the quantity $(2A_0 + \varepsilon_0)$ times the product of the detector efficiencies.

The quantity $2A_0 + \varepsilon_0$ is obtained from the measured coincidence rate N_{cB} as a function of the average pump beam power when one of the interferometer arms is blocked. The theoretical coincidence rate for this case is obtained by considering in the input of the BS only one propagation photon mode (a or b) and therefore, using the correlation function shown in Eq. (34) or (35). We then obtain

$$N_{cB} = N^2 E_p^4 \alpha_1 \alpha_2 (2A_0 + \varepsilon_0) = \alpha_1 \alpha_2 (2A_0 + \varepsilon_0) \left(\frac{P}{h\nu} \right)^2. \quad (56)$$

This coincidence rate, detected with one of the interferometer arms blocked, in terms of the average pump beam power is shown in Fig. 3. The continuous curve is an experimental fit done with the function cP^d ; $c=(4.9 \pm 0.2) \times 10^3$ photons/s W^2 and $d=2.00 \pm 0.02$ [see Eq. (56)]. We determine from c the quantity $2A_0 + \varepsilon_0$ times the product of the detector efficiencies.

The overall detection efficiency (that takes into account the interference filter transmission, pinhole area, and detector lens coupling), is deduced from the measured coincidence rate at the HOM interferometer exit for photon pairs in the singlet state for low pump beam power. Assuming that in this regime the two pair generation by SPDC is negligible, the theoretical coincidence rate becomes

$$\begin{aligned} N_c(\delta) &= N \frac{E_p^2}{2} X_0 \alpha_1 \alpha_2 (1 + e^{-(\Delta\omega_p)^2 \delta^2}) \\ &= \left(\frac{P}{h\nu} \right) \frac{X_0}{2} \alpha_1 \alpha_2 (1 + e^{-(\Delta\omega_p)^2 \delta^2}). \end{aligned} \quad (57)$$

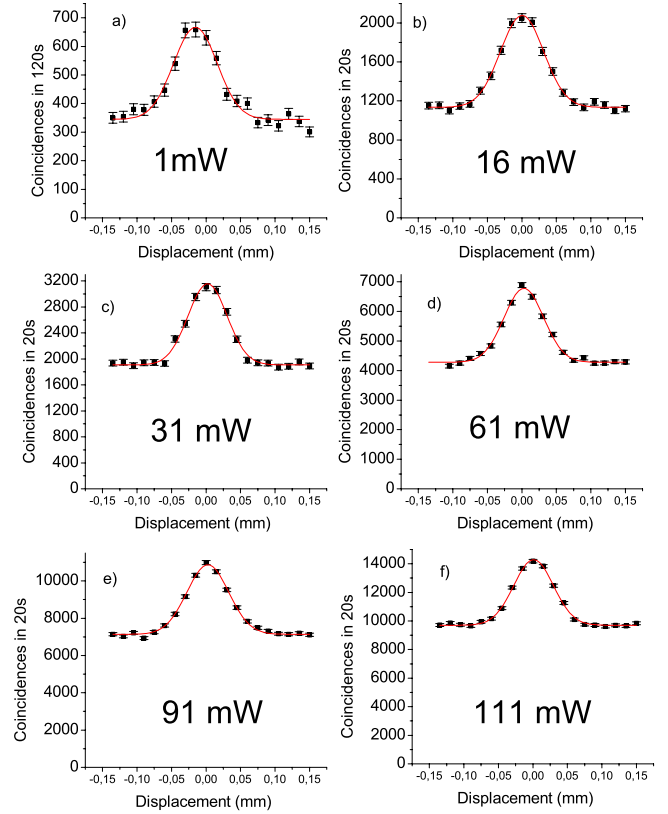


FIG. 4. (Color online) Experimental results of the coincidence rates for Hong-Ou-Mandel interferometer with two and four photons in a singlet state by phase-matching type II for different average pump beam powers: (a) 1 mW, (b) 16 mW, (c) 31 mW, (d) 61 mW, (e) 91 mW, and (f) 111 mW. The continuous curve is derived from Eq. (53).

We use the HOM plot shown in Fig. 4(a) that was obtained with 1 mW average pump beam power for obtaining the overall detector efficiency. For simplicity we assume that both detectors have the same detection efficiency. The quantities E_p^2 and $\alpha_i X_0$ in Eq. (57) are obtained from the average pump beam power and the single counts plot, respectively. Then, the theoretical fit of Fig. 4(a) with Eq. (57) gives us the detector efficiency $\alpha_i = (9.0 \pm 0.6) \times 10^{-3}$ that is used for obtaining experimentally X_0 and $2A_0 + \varepsilon_0$.

Finally the experimental coincidence rates in terms of the average pump beam power for photon pairs in the singlet state is plotted in Fig. 4. The continuous curve is derived from Eq. (53). We can also derive the dependence of the interference pattern visibility in terms of E_p^2 (proportional to the average pump beam power). The visibility is given by the following expression [25]:

$$v = \frac{N_c(0) - N_c(\infty)}{N_c(\infty)}, \quad (58)$$

and therefore

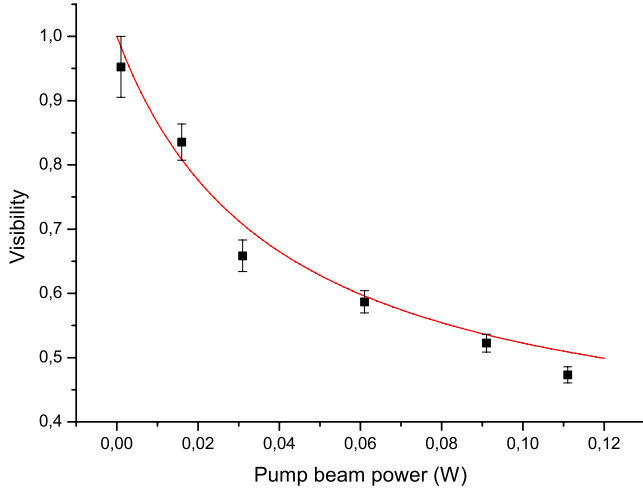


FIG. 5. (Color online) Measured visibility of the interference patterns shown in Fig. 4 as a function of the average pump beam power for photons in the singlet polarization state. The theoretical curve was obtained from Eq. (59) (continuous curve).

$$v = \frac{\frac{E_p^2 X_0}{2} + \frac{E_p^4}{4}(2A_0 + \varepsilon_0)}{\frac{E_p^2 X_0}{2} + \frac{3E_p^4}{4}(2A_0 + \varepsilon_0)} = 1 - \left(\frac{3}{2} + \frac{X_0}{E_p^2(2A_0 + \varepsilon_0)} \right)^{-1}, \quad (59)$$

where $N_c(\infty)$ means that the temporal delay δ is much larger than the longitudinal photon coherence length obtained from the HOM peak width. The measured visibility of the interference patterns shown in Fig. 4, as a function of the average pump beam power, are shown in Fig. 5. The continuous line is the theoretical curve obtained from Eq. (59). We notice a good agreement between the theoretical visibility curve and the HOM measured visibility points for photon pairs in the singlet state. All parameters in Eq. (59) were obtained as explained above and the experimental visibilities were obtained directly from the experimental curves (Fig. 4) following the visibility definition shown in Eq. (59). As it was predicted in Eq. (59) the visibility of the HOM interference pattern decreases when the average pump beam power increases since it increases the two pair generation rate. This behavior was observed theoretically by Nagasako *et al.* for the case of a parametric amplifier used as light source with photons with the same polarization being emitted [22]. Interference diagrams in their second work give a nice picture about the physics behind the visibility decrease when the gain in the parametric amplifier is increased [23]. In the low gain regime, only dual input modes (signal and idler) to the interferometer produce the coincidence counts and the destructive interference of the two possible output configurations that generate coincidences produces the dip. In the high gain regime, the single input modes (idler or signal) also generate coincidences decreasing the HOM dip visibility. Notice also in Eq. (59) that when the average pump power

tends to infinity the visibility tends to 1/3 and, when it is very small, the visibility tends to 1. The limiting visibility at large pump power of 1/3 is consistent with previous works where spatial interference from independent thermal sources were analyzed theoretically [30,31] and experimentally [32] with light generated by stimulated Raman scattering. Similar experiments have confirmed the decrease of an interference pattern visibility due to the increase of the multiphoton production [33].

IV. CONCLUSION

We used here the multimode frequency approach developed in Refs. [25,26] for studying the influence of the pump beam power in the interference pattern visibility of the Hong-Ou-Mandel interferometer. For the regime of strong pump beam power we must consider the spontaneous parametric generation of one and two photon pairs coming from one and two photons of the pump pulse, respectively. The coincidence rate at the exit of the interferometer is calculated as a function of the temporal photons' delay and of the pump beam power for photon pairs generated by a type I phase-matching crystal. The calculation is also extended to photon pairs generated by a type II phase-matching crystal when they are in a singlet or a triplet polarization state. An experiment was done for testing the calculation and a good agreement between theory and experimental results is demonstrated for the photon pairs exiting the crystal in a singlet polarization state. The theory and the experimental data show that by increasing the pump beam power the HOM interference pattern visibility decreases due to the increase of the two pairs generation per pulse.

ACKNOWLEDGMENTS

This work was supported by the Brazilian agencies CAPES, CNPq, and the Millennium Institute for Quantum Information. One of the authors (S.P.) thanks especially CAPES for support during a one year stay at the Università di Roma “La Sapienza,” where the experiment was performed. F. De Martini and F. Sciarrino acknowledge financial support from the MIUR (PRIN 2005) and from CNISM (Progetto Innesco 2006). One of the authors (F.A.B.) acknowledges EC-FET QAP-2005-015848. We thank Giorgio Milani and Sandro Giacomini for helping with the experiment setup. We would like to thank C. Olindo and A. Delgado for discussions.

APPENDIX: CALCULATION OF THE CORRELATION FUNCTION (9)

We start by calculating $\hat{\mathbf{F}}_b^{(+)}(t_2 - \delta)\hat{\mathbf{F}}_a^{(+)}(t_1 + \delta)|\psi\rangle$,

$$\begin{aligned}
\hat{\mathbf{F}}_b^{(+)}(t_2 - \delta)\hat{\mathbf{F}}_a^{(+)}(t_1 + \delta)|\psi\rangle &= \frac{\eta E_p}{2\pi} \int \int \int \int d\omega d\omega' d\omega_1 d\omega_2 e^{-i\omega(t_2 - \delta)} e^{-i\omega'(t_1 + \delta)} \Phi(\omega_1, \omega_2) \hat{b}(\omega) \hat{a}(\omega') \hat{a}^\dagger(\omega_1) \hat{b}^\dagger(\omega_2) |\text{vac}\rangle \\
&+ \frac{\eta^2 E_p^2}{4\pi} \int \int \int \int \int \int d\omega d\omega' d\omega_1 d\omega_2 d\omega'_1 d\omega'_2 e^{-i\omega(t_2 - \delta)} e^{-i\omega'(t_1 + \delta)} \Phi(\omega_1, \omega_2) \Phi(\omega'_1, \omega'_2) \\
&\times \hat{b}(\omega) \hat{a}(\omega') \hat{a}^\dagger(\omega'_1) \hat{b}^\dagger(\omega'_2) \hat{a}^\dagger(\omega_1) \hat{b}^\dagger(\omega_2) |\text{vac}\rangle.
\end{aligned} \tag{A1}$$

By using the commutation relations Eq. (17) in Eq. (A1) we obtain

$$\begin{aligned}
\hat{\mathbf{F}}_b^{(+)}(t_2 - \delta)\hat{\mathbf{F}}_a^{(+)}(t_1 + \delta)|\psi\rangle &= \frac{\eta E_p}{2\pi} \int \int d\omega_1 d\omega_2 e^{-i\omega_2(t_2 - \delta)} e^{-i\omega_1(t_1 + \delta)} \Phi(\omega_1, \omega_2) |\text{vac}\rangle \\
&+ \frac{\eta^2 E_p^2}{4\pi} \int \int \int \int d\omega_1 d\omega_2 d\omega'_1 d\omega'_2 \Phi(\omega_1, \omega_2) \Phi(\omega'_1, \omega'_2) [\hat{a}^\dagger(\omega_1) \hat{b}^\dagger(\omega_2) e^{-i\omega_2(t_2 - \delta)} e^{-i\omega_1(t_1 + \delta)} \\
&+ \hat{a}^\dagger(\omega_1) \hat{b}^\dagger(\omega'_2) e^{-i\omega_2(t_2 - \delta)} e^{-i\omega'_1(t_1 + \delta)} + \hat{a}^\dagger(\omega'_1) \hat{b}^\dagger(\omega_2) e^{-i\omega'_2(t_2 - \delta)} e^{-i\omega_1(t_1 + \delta)} \\
&+ \hat{a}^\dagger(\omega'_1) \hat{b}^\dagger(\omega'_2) e^{-i\omega_2(t_2 - \delta)} e^{-i\omega_1(t_1 + \delta)}] |\text{vac}\rangle,
\end{aligned} \tag{A2}$$

and the square modulus becomes

$$\begin{aligned}
|\hat{\mathbf{F}}_b^{(+)}(t_2 - \delta)\hat{\mathbf{F}}_a^{(+)}(t_1 + \delta)|\psi\rangle|^2 &= \frac{\eta^2 E_p^2}{4\pi^2} \int \int \int \int d\bar{\omega}_1 d\bar{\omega}_2 d\omega_1 d\omega_2 \Phi^*(\bar{\omega}_1, \bar{\omega}_2) \Phi(\omega_1, \omega_2) e^{-i(\omega_2 - \bar{\omega}_2)(t_2 - \delta)} e^{-i(\omega_1 - \bar{\omega}_1)(t_1 + \delta)} \\
&+ \frac{\eta^4 E_p^4}{16\pi^2} \int \int \int \int d\bar{\omega}_1 d\bar{\omega}_2 d\omega'_1 d\omega'_2 \int \int \int \int d\omega_1 d\omega_2 d\omega'_1 d\omega'_2 \Phi^*(\bar{\omega}_1, \bar{\omega}_2) \\
&\times \Phi^*(\omega'_1, \omega'_2) \Phi(\omega_1, \omega_2) \Phi(\omega'_1, \omega'_2) [\hat{a}(\bar{\omega}_1) \hat{b}(\bar{\omega}_2) \hat{a}^\dagger(\omega_1) \hat{b}^\dagger(\omega_2) e^{-i(\omega'_2 - \bar{\omega}_2)(t_2 - \delta)} e^{-i(\omega'_1 - \bar{\omega}_1)(t_1 + \delta)} + \dots].
\end{aligned} \tag{A3}$$

Then we employ the commutation relations Eq. (17) in Eq. (A3) and integrate over t_1 and t_2 in all times, since the photons' longitudinal coherence time is much smaller than the time resolution of the detection system. If we use the result (18) in the calculation, we obtain

$$\begin{aligned}
&= \eta^2 E_p^2 \int \int \int \int d\bar{\omega}_1 d\bar{\omega}_2 d\omega_1 d\omega_2 \delta(\omega_2 - \bar{\omega}_2) \delta(\omega_1 - \bar{\omega}_1) \Phi^*(\bar{\omega}_1, \bar{\omega}_2) \Phi(\omega_1, \omega_2) \\
&+ \frac{\eta^4 E_p^4}{4} \int \int \int \int d\bar{\omega}_1 d\bar{\omega}_2 d\omega'_1 d\omega'_2 \int \int \int \int d\omega_1 d\omega_2 d\omega'_1 d\omega'_2 \Phi(\omega_1, \omega_2) \Phi(\omega'_1, \omega'_2) \Phi^*(\bar{\omega}_1, \bar{\omega}_2) \\
&\times \Phi^*(\omega'_1, \omega'_2) 4[\delta(\bar{\omega}_1 - \omega_1) \delta(\bar{\omega}_2 - \omega_2) \delta(\omega'_2 - \bar{\omega}_2) \delta(\omega'_1 - \bar{\omega}_1) + \delta(\bar{\omega}_1 - \omega'_1) \delta(\bar{\omega}_2 - \omega_2) \delta(\omega'_2 - \bar{\omega}_2) \delta(\omega_1 - \bar{\omega}_1) \\
&+ \delta(\bar{\omega}_1 - \omega_1) \delta(\bar{\omega}_2 - \omega'_2) \delta(\omega_2 - \bar{\omega}_2) \delta(\omega'_1 - \bar{\omega}_1) + \delta(\bar{\omega}_1 - \omega'_1) \delta(\bar{\omega}_2 - \omega'_2) \delta(\omega_2 - \bar{\omega}_2) \delta(\omega_1 - \bar{\omega}_1)].
\end{aligned} \tag{A4}$$

The contribution of Eq. (9) to $N_{\text{Ic}}(\delta)$ is then

$$\begin{aligned}
&\eta^2 E_p^2 \int \int d\omega_1 d\omega_2 |\Phi(\omega_1, \omega_2)|^2 + 2\eta^4 E_p^4 \int \int \int \int d\omega_1 d\omega_2 d\omega'_1 d\omega'_2 [|\Phi(\omega_1, \omega_2)|^2 |\Phi(\omega'_1, \omega'_2)|^2 \\
&+ \Phi^*(\omega'_1, \omega_2) \Phi^*(\omega_1, \omega'_2) \Phi(\omega_1, \omega_2) \Phi(\omega'_1, \omega'_2)]
\end{aligned} \tag{A5}$$

or

$$\eta^2 E_p^2 + 2E_p^4 (A + \varepsilon). \tag{A6}$$

where A and ε were defined before in Eqs. (20) and (21).

- [1] A. Einstein, B. Podolski, and N. Rosen, *Phys. Rev.* **47**, 777 (1935).
- [2] Z. Y. Ou and L. Mandel, *Phys. Rev. Lett.* **61**, 50 (1988).
- [3] Y. H. Shih and C. O. Alley, *Phys. Rev. Lett.* **61**, 2921 (1988).
- [4] J. G. Rarity and P. R. Tapster, *Phys. Rev. Lett.* **64**, 2495 (1990).
- [5] T. E. Kiess, Y. H. Shih, A. B. Sergienko, and C. O. Alley, *Phys. Rev. Lett.* **71**, 3893 (1993).
- [6] D. M. Greenberger, M. A. Horne, A. Shimonye, and A. Zeilinger, *Am. J. Phys.* **58**, 1131 (1990); N. D. Mermin, *Phys. Rev. Lett.* **65**, 1838 (1990).
- [7] D. Bouwmeester, J. W. Pan, M. Daniell, H. Weinfurter, and A. Zeilinger, *Phys. Rev. Lett.* **82**, 1345 (1999); K. J. Resch, P. Walther, and A. Zeilinger, *ibid.* **94**, 070402 (2005).
- [8] L. Mandel and E. Wolf, *Optical Coherence and Quantum Optics* (Cambridge University Press, Cambridge, 1995).
- [9] J. G. Rarity, P. R. Tapster, and R. Loudon, in *Quantum Interferometry*, edited by F. D. Martini, G. Denardo, and Y. Shih (VCH, Weinheim, 1996); A. Kuzmich, I. A. Walmsley, and L. Mandel, *Phys. Rev. Lett.* **85**, 1349 (2000); D. Bouwmeester, J.-W. Pan, K. Mattle, M. Eibl, H. Weinfurter, and A. Zeilinger, *Nature (London)* **390**, 575 (1997); T. E. Keller, M. H. Rubin, and Y. Shih, *Phys. Lett. A* **244**, 507 (1998); C. Santori, D. Fattal, J. Vuckovic, G. S. Solomon, and Y. Yamamoto, *Nature (London)* **419**, 594 (2002); H. de Riedmatten, I. Marcikic, W. Tittel, H. Zbinden, and N. Gisin, *Phys. Rev. A* **67**, 022301 (2003); R. Kaltenbaek, B. Blauensteiner, M. Zukowski, M. Aspelmeyer, and A. Zeilinger, *Phys. Rev. Lett.* **96**, 240502 (2006).
- [10] E. Knill, R. Laflamme, and G. J. Milburn, *Nature (London)* **409**, 46 (2001); P. Kok, W. J. Munro, K. Remoto, T. C. Ralph, J. P. Bowling, and G. J. Milburn, *Rev. Mod. Phys.* **79**, 135 (2007).
- [11] D. Bouwmeester, J.-W. Pan, K. Mattle, M. Eibl, H. Weinfurter, and A. Zeilinger, *Nature (London)* **390**, 575 (1997); D. Boschi, S. Branca, F. De Martini, L. Hardy, and S. Popescu, *Phys. Rev. Lett.* **80**, 1121 (1998); E. Lombardi, F. Sciarrino, S. Popescu, and F. De Martini, *ibid.* **88**, 070402 (2002); I. Marcikic, H. de Riedmatten, W. Tittel, H. Zbinden, and N. Gisin, *Nature (London)* **421**, 509 (2003); R. Ursin *et al.*, *ibid.* **430**, 849 (2004).
- [12] C. K. Hong, Z. Y. Ou, and L. Mandel, *Phys. Rev. Lett.* **59**, 2044 (1987).
- [13] Z. Y. Ou and L. Mandel, *Phys. Rev. Lett.* **61**, 50 (1988); Y. Shih and C. O. Alley, *ibid.* **61**, 2921 (1988).
- [14] A. M. Steinberg, P. G. Kwiat, and R. Y. Chiao, *Phys. Rev. Lett.* **71**, 708 (1993); C. Olindo, M. A. Sagioro, F. M. Matinaga, A. Delgado, C. H. Monken, and S. Pádua, *Opt. Commun.* **272**, 161 (2007).
- [15] A. M. Steinberg, P. G. Kwiat, and R. Y. Chiao, *Phys. Rev. Lett.* **68**, 2421 (1992).
- [16] P. G. Kwiat, A. M. Steinberg, and R. Y. Chiao, *Phys. Rev. A* **45**, 7729 (1992).
- [17] F. De Martini, G. Di Giuseppe, and S. Pádua, *Phys. Rev. Lett.* **87**, 150401 (2001).
- [18] S. P. Walborn, A. N. de Oliveira, S. Pádua, and C. H. Monken, *Phys. Rev. Lett.* **90**, 143601 (2003).
- [19] M. A. Sagioro, C. Olindo, C. H. Monken, and S. Pádua, *Phys. Rev. A* **69**, 053817 (2004).
- [20] T. B. Pittman, M. J. Fitch, B. C. Jacobs, and J. D. Franson, *Phys. Rev. A* **68**, 032316 (2003); J. L. O'Brien *et al.*, *Nature (London)* **426**, 264 (2003); J. L. O'Brien, G. J. Pryde, A. Gilchrist, D. F. V. James, N. K. Langford, T. Ralph, and A. G. White, *Phys. Rev. Lett.* **93**, 080502 (2004); S. Gasparoni, J. W. Pan, P. Walther, T. Rudolph, and A. Zeilinger, *ibid.* **93**, 020504 (2004); Z. Zhao, A. N. Zhang, Y. A. Chen, H. Zhang, J. F. Du, T. Yang, and J. W. Pan, *ibid.* **94**, 030501 (2005); N. K. Langford, T. J. Weinhold, R. Prevedel, A. Gilchrist, J. L. O'Brien, G. J. Tryde, and A. D. White, *ibid.* **95**, 210504 (2005); N. Kiesel, C. Schmid, U. Weber, R. Ursin, and H. Weinfurter, *ibid.* **95**, 210505 (2005).
- [21] F. Sciarrino, C. Sias, M. Ricci, and F. De Martini, *Phys. Rev. A* **70**, 052305 (2004); M. Ricci, F. Sciarrino, C. Sias, and F. De Martini, *Phys. Rev. Lett.* **92**, 047901 (2004); W. T. M. Irvine, A. L. Linares, M. J. A. de Dood, and D. Bouwmeester, *ibid.* **92**, 047902 (2004).
- [22] E. M. Nagasako, S. J. Bentley, R. W. Boyd, and G. S. Agarwal, *Phys. Rev. A* **64**, 043802 (2001).
- [23] E. M. Nagasako, S. J. Bentley, R. W. Boyd, and G. S. Agarwal, *J. Mod. Opt.* **49**, 529 (2002).
- [24] A. N. Boto, P. Kok, D. S. Abrams, S. L. Braunstein, C. P. Williams, and J. P. Dowling, *Phys. Rev. Lett.* **85**, 2733 (2000).
- [25] Z. Y. Ou, J.-K. Rhee, and L. J. Wang, *Phys. Rev. A* **60**, 593 (1999).
- [26] Z. Y. Ou, *Phys. Rev. A* **72**, 053814 (2005).
- [27] N. Boeuf *et al.*, *Opt. Eng.* **39**, 1016 (2000).
- [28] P. G. Kwiat, K. Mattle, H. Weinfurter, A. Zeilinger, A. V. Sergienko, and Y. Shih, *Phys. Rev. Lett.* **75**, 4337 (1995).
- [29] B. A. Saleh and M. C. Teich, *Fundamentals of Photonics* (John Wiley, New York, 1991).
- [30] L. Mandel, *Phys. Rev. A* **28**, 929 (1983).
- [31] B. Yurke and M. Potasek, *Phys. Rev. A* **36**, 3464 (1987).
- [32] S. J. Kuo, D. T. Smithey, and M. G. Raymer, *Phys. Rev. A* **43**, 4083 (1991).
- [33] V. Scarania, H. de Riedmatten, I. Marcikic, H. Zbinden, and N. Gisin, *Eur. Phys. J. D* **32**, 129 (2005); H. S. Eisenberg, G. Khoury, G. A. Durkin, C. Simon, and D. Bouwmeester, *Phys. Rev. Lett.* **93**, 193901 (2005).